

Original Article

Int J Oral Biol 44:115-123, 2019
 pISSN: 1226-7155 • eISSN: 2287-6618
<https://doi.org/10.11620/IJOB.2019.44.3.115>

Effects of 3,3',4,4',5-pentachlorobiphenyl on human Kv1.3 and Kv1.5 channels

Jong-Hui Kim[†], Soobeen Hwang[†], Seo-in Park[†], and Su-Hyun Jo^{*}

Department of Physiology, Institute of Bioscience and Biotechnology, BK21 Plus Graduate Program, Kangwon National University College of Medicine, Chuncheon 24341, Republic of Korea

Among the environmental chemicals that may be able to disrupt the endocrine systems of animals and humans are polychlorinated biphenyls (PCBs), a chemical class of considerable concern. PCB consists of two six-carbon rings linked by a single carbon bond, and theoretically, 209 congeners can form, depending on the number of chlorines and their location on the biphenyl rings. Furthermore, 3,3',4,4',5-pentachlorobiphenyl (PCB126) exposure also increases nitric oxide production and nuclear factor kappa-light-chain-enhancer of activated B cells binding activity in chondrocytes, thus contributing as an initiator of chondrocyte apoptosis and resulting in thymic atrophy and immunosuppression. This study identified whether cardiac and immune abnormalities from PCB126 were caused by the Kv1.3 and Kv1.5 channels. PCB126 did not affect either the steady-state current or peak current of the Kv1.3 and Kv1.5 channels. However, PCB126 right-shifted the steady-state activation curves of human Kv1.3 channels. These results suggest that PCBs can affect the heart in a way that does not block voltage-dependent potassium channels including Kv1.3 and Kv1.5 directly.


Keywords: 3,3',4,4',5-pentachlorobiphenyl, Kv1.3 channel, Kv1.5 channel

Introduction

Polychlorinated biphenyls (PCBs), organic chemicals, were toxic [1]. Among the environmental chemicals that may be able to disrupt the endocrine systems of animals and humans, the PCB were a chemical class of considerable concern [2]. Residue analysis of human adipose tissue, blood, and breast milk confirms that most individuals have been environmentally exposed to PCBs and contain measurable levels in the tissues [2]. Polychlorinated biphenyls consist of two six-carbon rings linked by a single carbon bond and theoretically 209 congeners can form, depending upon the number of chlorines and their location on the biphenyl rings [3].

PCB congeners are typical carcinogens [4,5], suppresses the immune system [6,7], althyroid function increase the risk of developing [8,9], and causing a decrease in the heart function such as hypertension [10–12]. PCB congeners exposure to maternal is induced fetal developmental disturbances [13]. PCB congeners having at 4 or more chlorines each have significant aryl hydrocarbon receptor (AhR)-activating potential [1,3]. Halogenated aromatic hydrocarbons and polycyclic aromatic hydrocarbons like to PCB can act as AhR ligands [14]. Stimulated AhR with ligand binds to AhR nuclear translocator (ARNT) and function as a transcription factor *in vivo* [14]. This transcription factor binds to a specific DNA regulatory region, such as AhR-response element (Arnt), dioxin-response element

Received August 20, 2019; Revised September 15, 2019; Accepted September 18, 2019

*Correspondence to: Su-Hyun Jo, E-mail: suhyunjo@kangwon.ac.kr  <https://orcid.org/0000-0002-4090-9580>

[†]Jong-Hui Kim, Soobeen Hwang, and Seo-in Park contributed equally to this work.

Copyright © The Korean Academy of Oral Biology

© This is an open-access article distributed under the terms of the Creative Commons Attribution Non-Commercial License (<http://creativecommons.org/licenses/by-nc/4.0/>), which permits unrestricted non-commercial use, distribution, and reproduction in any medium, provided the original work is properly cited.

and xenobiotics–response element, promoting the expression of abnormal genes, thereby induced toxicity [15]. In addition, Protein produced by stimulation of the AhR produces intermediary metabolites that have toxic, directly damage DNA, during the synthesis [16].

3,3',4,4',5–pentachlorobiphenyl (PCB126) (Fig. 1) was a dioxin–like PCB and a potent AhR agonist [17]. Specificity of PCB126 actions on the G protein coupled receptor pathway was shown by normal burst oxidative activation evoked by toll–like receptor 4 and protein kinase C direct activation [18]. PCB126 was a cardiovascular risk factor that increases the heart weight and serum cholesterol levels in female rats [19]. PCB126 exposure also increased nitric oxide production and nuclear factor kappa–light–chain–enhancer of activated B cells binding activity in the chondrocytes, and may be an initiator of chondrocyte apoptosis, which is closely linked to degradation of cartilage in osteoarthritis pathogenesis [20]. Also PCB126 produces thymic atrophy and immunosuppression [21].

The study identified whether cardiac and immune abnormalities with PCB126 were caused by K^+ channels. Voltage–dependent K^+ channels (Kv) conduct K^+ ions across the cell membrane in response to changes in the membrane voltage, thereby regulating neuronal excitability by modulating the shape and frequency of action potentials [22]. Kv channels, a superfamily comprised of 12 subfamilies (Kv1–Kv12), are involved in a number of physiological processes, were typically closed at the resting potential of the cell, but open on membrane depolarization [23]. Kv1.5 and Kv1.3, the voltage dependent K^+ channels, are members of the Kv1 Shaker family of K^+ channels, which are involved in tissue differentiation and cell growth [24].

Kv1.3 channel is a delayed–rectifier channel and shows slow C–type inactivation by changing the selectivity filter [25]. Kv1.3 channel is encoded by the *KCNA3* gene and is specifically expressed in the central nervous system, osteoclast, and T cell, and is functional in producing human vascular smooth muscle cells [26]. Kv1.3 channel regulates membrane potential and Ca^{2+} signaling in human T cells, and its expression is increased

4– to 5–fold in activated CD4+ and CD8+ TEM/TEMRA cells [27]. The activity of the Kv1.3 channel is the K^+ that goes out of the cell and becomes hyperpolarized [28]. When the intracellular charge falls to a negative charge, the Ca^{2+} is introduced, thereby promoting activation of Ca^{2+} dependent transcription factors and induction of T lymphocyte proliferation [28]. The Kv1.3 channel is considered a potential target for immune diseases for these reasons [29].

In heart, Kv1.5 channels determine the resting potential, shape, and length of the action potential, thus controlling cardiac performance [30]. The present work shows that arachidonic acid and some other long chain polyunsaturated fatty acids such as docosahexaenoic acid, which is abundant in fish oil, produce a direct open channel block of the major Kv1.5 cloned in cardiac cells [31]. The suppression of Kv1.5 channels inhibit delayed rectified K^+ channels in myocardial cells and was important in processes such as long–term potentiation or depression [31].

In this study, I have analyzed the electrophysiological effects of PCB126 on human Kv1.5 and Kv1.3 channels expressed in *Xenopus* oocytes and a two–microelectrode voltage clamp amplifier. We consider the effects of PCB126 on Kv1.3 and Kv1.5 channel currents and determine the physiological and pharmacological meaning of these effects.

Materials and Methods

1. Expression of Kv1.3 and Kv1.5 in oocytes

Human Kv1.3 (GenBank accession no. BC035059.1) cRNA and Kv1.5 (hKv1.5, GenBank accession no. BC099665.3) cRNA were synthesized by *in vitro* transcription using Message Machine T7 kits (Ambion, Austin, TX, USA) and stored in nuclease–free water at -80°C . Stage V and VI oocytes were surgically eliminated from female *Xenopus laevis* (Nasco, Modesto, CA, USA) anesthetized with ice for 30 minutes at 10 minutes interval, and isolated from theca and follicle layers using fine forceps. After two days removal of theca and follicle, *Xenopus* oocytes were injected with 20 nL cRNA (0.4 $\mu\text{g}/\mu\text{L}$). These procedures were implemented under the Research Guidelines of Kangwon National University IACUC. Injected oocytes were maintained at 17°C in modified Barth's Solution, which was composed of (mM): 88 NaCl, 1 KCl, 0.4 CaCl, 0.33 $\text{Ca}(\text{NO}_3)_2$, 1 MgSO_4 , 2.4 NaHCO_3 , 10 HEPES (pH 7.4), and 50 $\mu\text{g}/\text{mL}$ gentamicin sulfate. Currents were measured 4 to 5 days after injection.

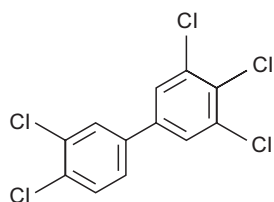


Fig. 1. Structure of 3,3',4,4',5–pentachlorobiphenyl (PCB126).

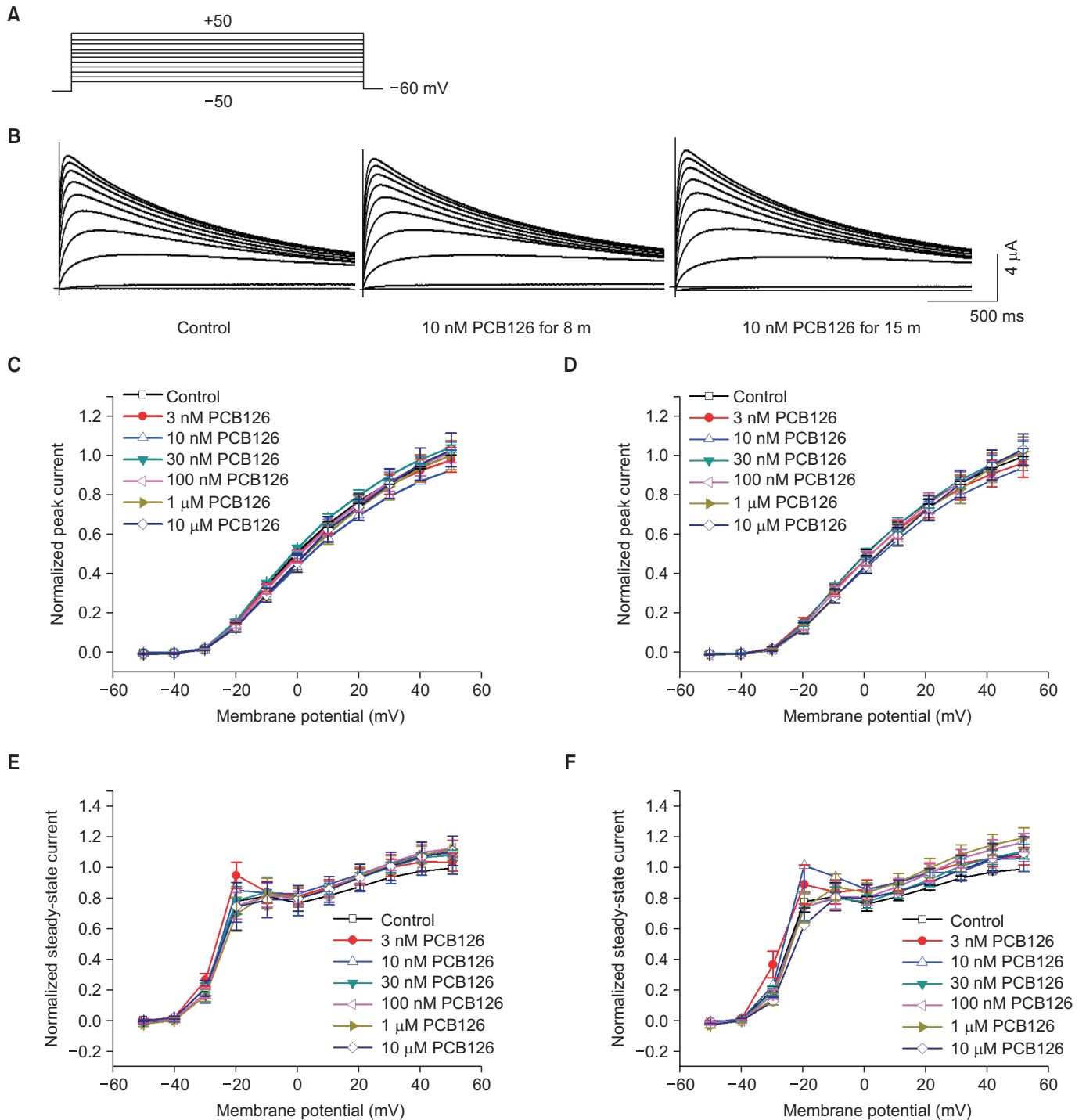


Fig. 2. Effect of 3,3',4,4',5-pentachlorobiphenyl (PCB126) on Kv1.3 channel currents. (A) Voltage pulses from -50 mV to $+50$ mV of 1 seconds duration with 10 mV increments every 10 seconds from a holding potential of -60 mV. (B) Superimposed current traces for exposure to not be exposed to PCB126 and 10 nM PCB126 for 8 minutes and for 15 minutes. Current-voltage (I-V) relationship of peak and steady-state currents of human Kv1.3 channel in the deficiency and exposure to of 3 nM, 10 nM, 30 nM, 100 nM, 1 μ M, and 10 μ M PCB126 for (C, E) 8 minutes or (D, F) 15 minutes. Peak currents were identified at the highest current and Steady-state currents were identified at the finish of depolarizing pulses. Peak currents and steady-state currents of $+50$ mV in not exposed to PCB126 were normalized to 1. Symbols with error bars present mean \pm standard error of the mean (n = 5-11).

2. Voltage-clamp recording from oocytes.

ND96 solution, which was composed of (mM): 96 NaCl, 2 KCl, 1.8 CaCl₂, 1 MgCl₂, and 10 HEPES (pH7.4), was used to oocytes by constant perfusion of the experimental bath chamber, and solution exchanges were concluded within 3 or 4 minutes. Currents were measured 8 minutes and 15 minutes after solution exchange at room temperature (20–23°C) with two-microelectrode voltage clamp systems (Warner Instruments, Hamden, CT, USA). Electrodes were filled with 3 M KCl with a resistance of 2.0–4.0 MΩ for voltage-recording electrodes and 2.0–2.5 MΩ for current-passing electrodes. Stimulation and data acquisition were regulated with an AD–DA converter (Axon Instruments Digidata 1200; Molecular Devices, San Jose, CA, USA) and pCLAMP software v5.1 (Molecular Devices). Stock solutions of 3 nM, 10 nM, 30 nM, 100 nM, 300 nM, 1 μM, 2 μM, 5 μM, and 10 μM, PCB126 were dissolved in dimethyl sulfoxide and added to the ND96 solution at suitable concentrations shortly before each experiment. PCB126 was purchased from ChemSpider (Raleigh, NC, USA) and other reagents were purchased from Sigma–Aldrich (St. Louis, MO, USA).

3. Data analysis

Origin 8.0 (OriginLab Co., Northampton, MA, USA) software was used for data acquisition and analysis. Concentration-dependent current inhibition data were fitted to a Hill equation as follows:

$$y = 1 / [1 + (IC_{50} / [D])^n]$$

IC₅₀ was the concentration at which half-maximal currents were inhibited and [D] was PCB126 concentration. Activation phase current trace was fitted with a single exponential function, respectively, which was considered the dominant time constant. Steady-state activation curves were obtained by fitting the data to a Boltzmann equation:

$$y = 1 / \{1 + \exp [-(V - V_{1/2}) / k]\}$$

V was the test potential. V_{1/2} was the half-activation potential (voltage at which the conductance was half-activated) and k was the slope factor. All data are expressed as mean ± SEM. Paired student's *t*-tests or ANOVA were used for statistical comparisons. Differences were considered significant at *p* <

0.05.

Results

1. Effects of PCB126 on human Kv1.3 channel currents

The effects of PCB126 on Kv1.3 channel currents were measured using *Xenopus* oocytes expression system. We exposed the control solution to *Xenopus* oocytes to normalize the peak amplitude. Fig. 2. shows peak currents and steady-state currents recordings of voltage clamps in *Xenopus* to control

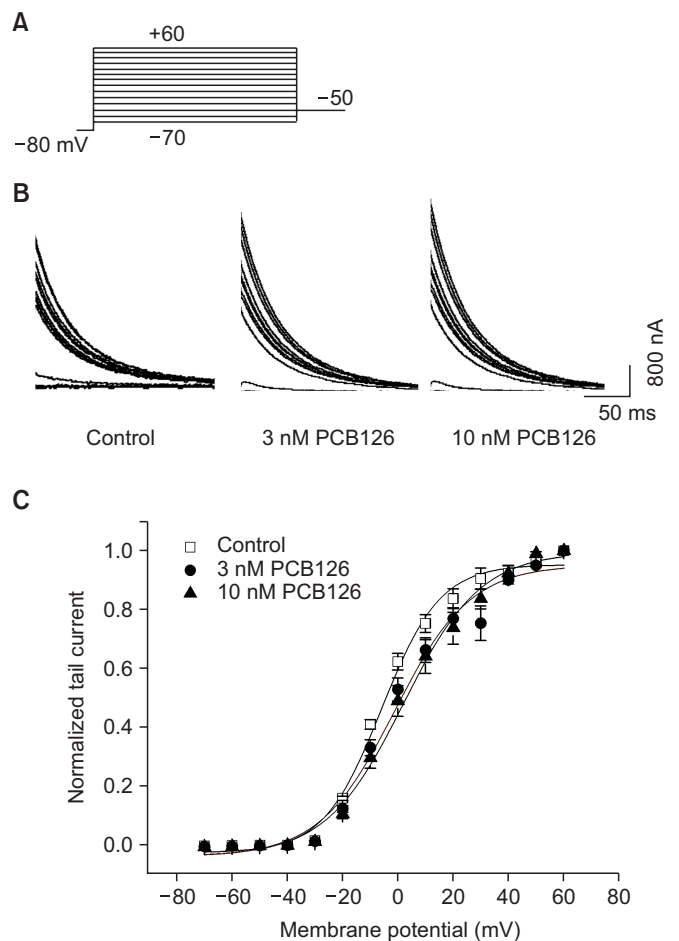


Fig. 3. Effect of PCB126 on steady-state activation of Kv1.3 channels. (A) Representative steady-state activation tail currents recorded at -50 mV after 100 ms depolarizing pulses from -70 to +60 mV in the absence and presence of 3 nM and 10 nM PCB126. (B) Superimposed steady-state activation current traces processed with control, 3 nM PCB126, and 10 nM PCB126. (C) Steady-state activation curves were obtained by normalizing each tail current when depolarized to +60 mV by fitting data with a Boltzmann equation. Symbols with error bars present mean ± standard error of the mean (n = 5–7).

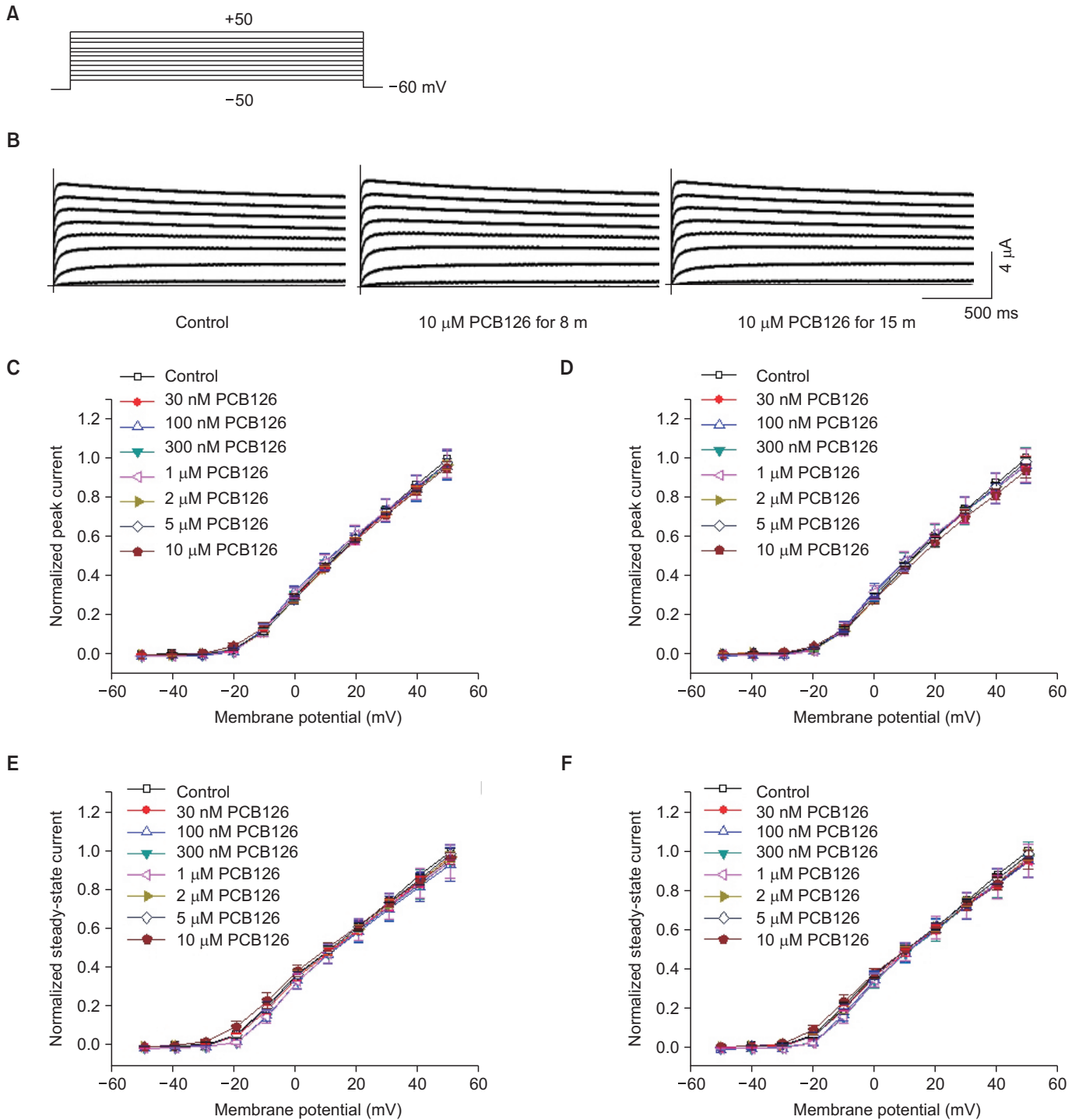


Fig. 4. Effect of PCB126 on Kv1.5 channel currents. (A) Voltage pulses from -50 mV to $+50$ mV of 1 second duration with 10 mV increments every 10 seconds from a holding potential of -60 mV. (B) Superimposed current traces for exposure to not exposed to PCB126 and $10 \mu\text{M}$ PCB126 for 8 minutes and for 15 minutes. Current-voltage (I - V) relationship of peak and steady-state currents of human Kv1.5 channel in the deficiency and exposure to of 30 nM, 100 nM, 300 nM, 1 μM , 2 μM , 5 μM , and 10 μM PCB126 for (C, E) 8 minutes or (D, F) 15 minutes. Peak currents were identified at the highest current and steady-state currents were identified at the finish of depolarizing pulses. Peak currents and steady-state currents of $+50$ mV in to not exposed to PCB126 were normalized to 1. Symbols with error bars present mean \pm standard error of the mean ($n = 5-11$).

conditions exposed only to ND96 solution and after exposure to 3 nM, 10 nM, 30 nM, 100 nM, 1 μ M, and 10 μ M PCB126 for 8 and 15 minutes on human Kv1.3 channel currents. PCB126 did not affect either the steady-state current or peak current of Kv1.3 channel ($n = 5-11$) (Fig. 2).

2. Effects of PCB126 on steady-state activation of Kv1.3 channels

To obtain whether PCB126 affected the activation kinetics of Kv1.3 channel currents, two-pulse protocols were used to evoke tail currents (Fig. 3). Steady-state activation curves were obtained from normalized tail currents (Fig. 3B) and fitted by two different Boltzmann equations. In the absence of PCB126, half-activation potential ($V_{1/2}$) in the activation curve was -1.74 ± 1.26 mV, and slope value (k) were 13.92 ± 0.67 ($n = 5-7$) (Fig. 3C). Exposure to 3 nM PCB126 changed $V_{1/2}$ to 3.64 ± 1.18 mV and slope value (k) to 14.76 ± 0.51 ($n = 5-7$) (Fig. 4C). Also $V_{1/2}$ and k -values increased to 9.44 ± 2.44 mV and 16.34 ± 1.09 , respectively by 10 nM PCB126 in human Kv1.3 channel currents ($n = 5-7$) (Fig. 3C). These results suggest that PCB126 right-shifted the steady-state activation curves of human Kv1.3 channels ($n = 5-7$) (Fig. 3C) ($p < 0.05$).

3. Effects of PCB126 on human Kv1.5 channel currents

The effects of PCB126 on Kv1.5 channel currents were measured using *Xenopus* oocytes expression system. We exposed the ND96 solution to *Xenopus* oocytes to normalize the peak amplitude. Fig. 4. shows peak currents and steady-state currents recordings of voltage clamps in *Xenopus* to control conditions exposed only to ND 96 solution and after exposure to 30 nM, 100 nM, 300 nM, 1 μ M, 2 μ M, 5 μ M, and 10 μ M PCB126 for 8 (Fig. 4 C and 4E) and 15 minutes (Fig. 4D and 4F) on human Kv1.5 channel currents. PCB126 did not affect either the steady-state current or peak current of Kv1.5 channel ($n = 5-11$) (Fig. 4).

Discussion

PCBs are persistent environmental pollutants that elicit a number of adverse health effects including teratogenesis, neurotoxicity, immunotoxicity, reproductive toxicity, endocrine disruption, and carcinogenesis [32]. PCB126 supposed one of the most potent dioxin-like and AhR agonist [17]. PCB126 and

AhR activation disrupt actin/myosin interaction to cause the prototypical cardiotoxicity [33].

Fig. 2. shows peak currents and steady-state currents recordings of voltage clamps in *Xenopus* to control conditions exposed only to ND96 solution and after exposure PCB126 on human Kv1.3 and Kv1.5 channel currents. PCB126 did not affect either the steady-state current or peak current of Kv1.3 and Kv1.5 channel (Fig. 2). $V_{1/2}$ of the activation curve was -1.74 ± 1.26 mV. k -value was 13.92 ± 0.67 in the absence of PCB126. Exposure to 3 nM PCB126 changed $V_{1/2}$ to 3.64 ± 1.18 mV and k -value to 14.76 ± 0.51 ($n = 5-7$) (Fig. 3C). Also, $V_{1/2}$ and k -value increased to 9.44 ± 2.44 mV and 16.34 ± 1.09 by 10 nM PCB126, respectively ($n = 5-7$) (Fig. 3C). PCB126 at 3–10 nM increased the $V_{1/2}$ compared with control, indicating right-shift of the steady-state activation curves by PCB126 ($n = 5-7$) (Fig. 3C) ($p < 0.05$). However, the increase in PCB126 concentration from 3 nM to 10 nM did not change the $V_{1/2}$ of steady-state activation curves ($n = 5-7$) (Fig. 3C) ($p > 0.05$). These results suggest that PCB126 could make activation of Kv1.3 channel.

Kv channels are regulated by a variety of stimuli of membrane voltage, protein phosphorylation, intracellular Ca^{2+} and accessory proteins [34,35]. Phosphatidylinositol 4,5-bisphosphate (PIP_2) a phospholipid, is also known to be a regulator of the Kv channel [36]. PIP_2 can directly regulate the gating of the Kv channel by directly binding to the channel structure, and generates a second messenger such as diacylglycerol (DAG) and inositol 1,4,5-trisphosphate (IP_3) by cleavage of PIP_2 by phospholipase C [36]. DAG and IP_3 activate enzymes such as protein kinase C to increase intracellular Ca^{2+} ions [37]. Studies have shown that PIP_2 directly regulates some Kv channels [38]. In particular, the addition of PIP_2 to the cytoplasm significantly increases the amplitude of the current due to almost no inactivation of the Kv1.3 and Kv1.5 channels [25]. PIP_2 eliminated $Kv\beta 1.3$ -induced N-type fast inactivation of Kv1.5 measured in inside-out macro-patches from *Xenopus* oocytes [25]. PIP_2 antagonized Kv1.5 inactivation by $Kv\beta 1.3$ in a concentration-dependent manner [25]. We confirmed the activation curve right-shift of the Kv1.3 channel, however, PIP_2 was shifted the activation curve to the negative side [25]. In addition, PCB126 did not affect the amplitude of Kv1.3 and Kv1.5 channels in our study. On the contrary, PIP_2 significantly affected the amplitude of Kv1.3 and Kv1.5 channel currents [25]. Therefore, we could exclude the hypothesis that PCB126 could block Kv1.3 channels by stimulating PIP_2 .

Kv1.3 channel promote the sustained Ca^{2+} influx necessary

for complete T cell activation, and are highly expressed in TEM cells and regulate their activity [39]. Kv1.3 channel is functional in generating human vascular smooth muscle cells. Kv1.3 was one of the first voltage-gated potassium channels reported to be modulated during apoptosis and was shown to contribute to the increased K⁺ efflux underlying the late phase of lymphocyte apoptosis. Lack or down-regulation of expression of Kv1.3 in lymphocytes conferred resistance to apoptosis [40]. Kv1.3 channels are recognized as therapeutic targets for autoimmune diseases, but blockage of Kv1.3 may cause various diseases such as immune diseases, and is also closely related to the activation of other channels, which may lead to a combination of different problems.

The presence of PCBs in the environment presents various toxic effects *in vivo* and *in vitro*. The exposure of PCB126 right-shifted the steady-state activation curves of human Kv1.3 channels. These results suggest that PCBs could affect the heart in a way that did not block a voltage-dependent po-

tassium channel, Kv1.3 channel directly. We need more study related to the pharmacology and physiological mechanisms by which PCB126 blocks Kv1.3 channels.

Acknowledgements

We thank Prof. Han Chae, Ulsan University School of Medicine, for the gift of the Kv1.3, Kv1.5 and hERG cDNA. This research was supported by Basic Science Research Program through the National Research Foundation of Korea (NRF) funded by the Ministry of Education (NRF-2015R1D1A1A-01057549).

Conflicts of Interest

No potential conflict of interest relevant to this article was reported.

References

1. Inter-Organization Programme for the Sound Management of Chemicals. Guidelines for the identification of PCBs and materials containing PCBs. Geneva: UNEP Chemicals; 1999.
2. McKinney JD, Waller CL. Polychlorinated biphenyls as hormonally active structural analogues. *Environ Health Perspect* 1994;102:290-7. doi: 10.1289/ehp.94102290.
3. McFarland VA, Clarke JU. Environmental occurrence, abundance, and potential toxicity of polychlorinated biphenyl congeners: considerations for a congener-specific analysis. *Environ Health Perspect* 1989;81:225-39. doi: 10.1289/ehp.8981225.
4. Tharappel JC, Lee EY, Robertson LW, Spear BT, Glauert HP. Regulation of cell proliferation, apoptosis, and transcription factor activities during the promotion of liver carcinogenesis by polychlorinated biphenyls. *Toxicol Appl Pharmacol* 2002;179:172-84. doi: 10.1006/taap.2001.9360.
5. Oakley GG, Devanaboyina U, Robertson LW, Gupta RC. Oxidative DNA damage induced by activation of polychlorinated biphenyls (PCBs): implications for PCB-induced oxidative stress in breast cancer. *Chem Res Toxicol* 1996;9:1285-92. doi: 10.1021/tx960103o.
6. Jeon YJ, Youk ES, Lee SH, Suh J, Na YJ, Kim HM. Polychlorinated biphenyl-induced apoptosis of murine spleen cells is aryl hydrocarbon receptor independent but caspases dependent. *Toxicol Appl Pharmacol* 2002;181:69-78. doi: 10.1006/taap.2002.9389.
7. Tan Y, Li D, Song R, Lawrence D, Carpenter DO. Ortho-substituted PCBs kill thymocytes. *Toxicol Sci* 2003;76:328-37. doi:10.1093/toxsci/kfg233.
8. Koopman-Esseboom C, Morse DC, Weisglas-Kuperus N, Lutkeschipholt IJ, Van der Paauw CG, Tuinstra LG, Brouwer A, Sauer PJ. Effects of dioxins and polychlorinated biphenyls on thyroid hormone status of pregnant women and their infants. *Pediatr Res* 1994;36:468-73. doi: 10.1203/00006450-199410000-00009.
9. Hagmar L. Polychlorinated biphenyls and thyroid status in humans: a review. *Thyroid* 2003;13:1021-8. doi:10.1089/105072503770867192.
10. Baker EL Jr, Landrigan PJ, Glueck CJ, Zack MM Jr, Liddle JA, Burse VW, Housworth WJ, Needham LL. Metabolic consequences of exposure to polychlorinated biphenyls (PCB) in sewage sludge. *Am J Epidemiol* 1980;112:553-63. doi: 10.1126/science.7010603.
11. Wilsgaard T, Jacobsen BK, Schirmer H, Thune I, Løchen ML, Njølstad I, Arnesen E. Tracking of cardiovascular risk factors: the Tromsø study, 1979-1995. *Am J Epidemiol* 2001;154:418-26. doi: 10.1093/oxfordjournals.aje.a113024.
12. Jo SH, Choi SY, Kim KT, Lee CO. Effects of polychlorinated biphenyl 19 (2,2',6-trichlorobiphenyl) on contraction, Ca²⁺ transient, and Ca²⁺ current of cardiac myocytes. *J Cardiovasc*

- Pharmacol 2001;38:11–20. doi: 10.1093/aje/154.5.418.
13. Bardin CW, Catterall JF. Testosterone: a major determinant of extragenital sexual dimorphism. *Science* 1981;211:1285–94. doi: 10.1097/00005344-200107000-00002.
 14. Vondráček J, Machala M, Bryja V, Chramostová K, Krcmár P, Dietrich C, Hampl A, Kozubík A. Aryl hydrocarbon receptor-activating polychlorinated biphenyls and their hydroxylated metabolites induce cell proliferation in contact-inhibited rat liver epithelial cells. *Toxicol Sci* 2005;83:53–63. doi: 10.3390/toxins6030934.
 15. Hankinson O. The aryl hydrocarbon receptor complex. *Annu Rev Pharmacol Toxicol* 1995;35:307–40.
 16. Carpenter DO, Stoner CR, Lawrence DA. Flow cytometric measurements of neuronal death triggered by PCBs. *Neurotoxicology* 1997;18:507–13. doi: 10.1146/annurev.pa.35.040195.001515.
 17. Carpenter DO. Polychlorinated biphenyls (PCBs): routes of exposure and effects on human health. *Rev Environ Health* 2006;21:1–23. doi: 10.1515/REVEH.2006.21.1.1.
 18. Shimada AL, Cruz WS, Loiola RA, Drewes CC, Dörr F, Figueiredo NG, Pinto E, Farsky SH. Absorption of PCB126 by upper airways impairs G protein-coupled receptor-mediated immune response. *Sci Rep* 2015;5:14917. doi: 10.1038/srep-14917.
 19. Lind PM, Orberg J, Edlund UB, Sjöblom L, Lind L. The dioxin-like pollutant PCB126 (3,3',4,4',5-pentachlorobiphenyl) affects risk factors for cardiovascular disease in female rats. *Toxicol Lett* 2004;150:293–9. doi: 10.1016/j.toxlet.2004.02.008.
 20. Lee HG, Yang JH. PCB126 induces apoptosis of chondrocytes via ROS-dependent pathways. *Osteoarthritis Cartilage* 2012;20:1179–85. doi: 10.1016/j.joca.2012.06.004.
 21. Goff KF, Hull BE, Grasman KA. Effects of PCB126 on primary immune organs and thymocyte apoptosis in chicken embryos. *J Toxicol Environ Health A* 2005;68:485–500. doi: 10.1080/15287390590903720.
 22. Long SB, Campbell EB, Mackinnon R. Crystal structure of a mammalian voltage-dependent Shaker family K⁺ channel. *Science* 2005;309:897–903. doi: 10.1126/science.1116269.
 23. Felipe A, Vicente R, Villalonga N, Roura-Ferrer M, Martínez-Mármol R, Solé L, Ferreres JC, Condom E. Potassium channels: new targets in cancer therapy. *Cancer Detect Prev* 2006;30:375–85. doi: 10.1016/j.cdp.2006.06.002.
 24. Comes N, Bielanska J, Vallejo-Gracia A, Serrano-Albarrás A, Marruecos L, Gómez D, Soler C, Condom E, Cajal SR, Hernández-Losa J, Ferreres JC, Felipe A. The voltage-dependent K⁽⁺⁾ channels Kv1.3 and Kv1.5 in human cancer. *Front Physiol* 2013;4:283. doi: 10.3389/fphys.2013.00283.
 25. Decher N, Gonzalez T, Streit AK, Sachse FB, Renigunta V, Soom M, Heinemann SH, Daut J, Sanguinetti MC. Structural determinants of Kvbeta1.3-induced channel inactivation: a hairpin modulated by PIP2. *EMBO J* 2008;27:3164–74. doi: 10.1038/emboj.2008.231.
 26. Wei AD, Gutman GA, Aldrich R, Chandy KG, Grissmer S, Wulff H. International Union of Pharmacology. LII. Nomenclature and molecular relationships of calcium-activated potassium channels. *Pharmacol Rev* 2005;57:463–72. doi: 10.1124/pr.57.4.9.
 27. Beeton C, Wulff H, Standifer NE, Azam P, Mullen KM, Pennington MW, Kolski-Andreaco A, Wei E, Grino A, Counts DR, Wang PH, LeeHealey CJ, S Andrews B, Sankaranarayanan A, Homerick D, Roeck WW, Tehranzadeh J, Stanhope KL, Zimin P, Havel PJ, Griffey S, Knaus HG, Nepom GT, Gutman GA, Calabresi PA, Chandy KG. Kv1.3 channels are a therapeutic target for T cell-mediated autoimmune diseases. *Proc Natl Acad Sci U S A* 2006;103:17414–9. doi:10.1073/pnas.0605136103.
 28. Cahalan MD, Chandy KG. Ion channels in the immune system as targets for immunosuppression. *Curr Opin Biotechnol* 1997;8:749–56. doi: 10.1016/S0958-1669(97)80130-9.
 29. Anangi R, Koshy S, Huq R, Beeton C, Chuang WJ, King GF. Recombinant expression of margatoxin and agitoxin-2 in *Pichia pastoris*: an efficient method for production of KV1.3 channel blockers. *PLoS One* 2012;7:e52965. doi: 10.1371/journal.pone.0052965.
 30. Roberds SL, Tamkun MM. Developmental expression of cloned cardiac potassium channels. *FEBS Lett* 1991;284:152–4. doi: 10.1016/0014-5793(91)80673-Q.
 31. Honoré E, Barhanin J, Attali B, Lesage F, Lazdunski M. External blockade of the major cardiac delayed-rectifier K⁺ channel (Kv1.5) by polyunsaturated fatty acids. *Proc Natl Acad Sci U S A* 1994;91:1937–41. doi: 10.1073/pnas.91.5.1937.
 32. Safe S, Krishnan V. Cellular and molecular biology of aryl hydrocarbon (Ah) receptor-mediated gene expression. *Arch Toxicol Suppl* 1995;17:99–115. doi: 10.1007/978-3-642-79451-3_8.
 33. Erwin KN. Insights into PCB126/Aryl hydrocarbon receptor-induced developmental cardiotoxicity in zebrafish. *Ann Arbor: Duke University*; 2013:3605525.
 34. Vacher H, Trimmer JS. Diverse roles for auxiliary subunits in phosphorylation-dependent regulation of mammalian brain voltage-gated potassium channels. *Pflugers Arch* 2011;462:631–43. doi: 10.1007/s00424-011-1004-8.

35. Gamper N, Li Y, Shapiro MS. Structural requirements for differential sensitivity of KCNQ K⁺ channels to modulation by Ca²⁺/calmodulin. *Mol Biol Cell* 2005;16:3538–51. doi: 10.1091/mbc.E04-09-0849.
36. Kruse M, Hammond GR, Hille B. Regulation of voltage-gated potassium channels by PI(4,5)P₂. *J Gen Physiol* 2012;140:189–205. doi: 10.1085/jgp.201210806.
37. Jonas EA, Kaczmarek LK. Regulation of potassium channels by protein kinases. *Curr Opin Neurobiol* 1996;6:318–23. doi: 10.1016/S0959-4388(96)80114-0.
38. Bian JS, Kagan A, McDonald TV. Molecular analysis of PIP₂ regulation of HERG and IKr. *Am J Physiol Heart Circ Physiol* 2004;287:H2154–63. doi: 10.1152/ajpheart.00120.2004.
39. Wulff H, Calabresi PA, Allie R, Yun S, Pennington M, Beeton C, Chandy KG. The voltage-gated Kv1.3 K⁽⁺⁾ channel in effector memory T cells as new target for MS. *J Clin Invest* 2003;111:1703–13. doi: 10.1172/JCI16921.
40. Szabò I, Zoratti M, Gulbins E. Contribution of voltage-gated potassium channels to the regulation of apoptosis. *FEBS Lett* 2010;584:2049–56. doi: 10.1016/j.febslet.2010.01.038.